Analytic quadratic integration over the two-dimensional Brillouin zone

1988 J. Phys. C: Solid State Phys. 21 4263

(http://iopscience.iop.org/0022-3719/21/23/012)

J. Phys. C: Solid State Phys. **21** (1988) 4263–4283. Printed in the UK

Analytic quadratic integration over the two-dimensional Brillouin zone

G Wiesenekker, G te Velde and E J Baerends
Department of Theoretical Chemistry, Free University, De Boelelaan, 1081 HV Amsterdam, The Netherlands

Received 25 November 1987

Abstract. A new method is described to evaluate analytically integrals of quadratically interpolated functions over the two-dimensional Brillouin zone. The method is not geometric in nature like the quadratic method of Methfessel and co-workers, but is algebraic. It allows quadratic interpolation not only for the dispersion relation $\varepsilon_n(\boldsymbol{k})$, but for property functions $f_n(\boldsymbol{k})$ as well. Comparisons are made between the analytic quadratic integration and the commonly used analytic linear integration by calculating tight-binding Brillouin zone integrals with the same number of $\boldsymbol{k}$-points for both methods. It is shown that convergence behaviour and convergence rate are far better for the analytic quadratic integration than for the analytic linear integration. Roughly, analytic quadratic integration can achieve the same accuracy as analytic linear integration with only about the square root of the total number of $\boldsymbol{k}$-points needed.

1. Introduction

Calculation of properties of solids with m-dimensional ($m = 1, 2, 3$) translation symmetry requires evaluation of integrals such as

$$J(E) = \sum_n \int_V f_n(\boldsymbol{k})\theta(E - \varepsilon_n(\boldsymbol{k}))\, \mathrm{d}^m\boldsymbol{k} \tag{1}$$

and

$$I(E) = \frac{\mathrm{d}J(E)}{\mathrm{d}E} = \sum_n \int_V f_n(\boldsymbol{k})\delta(E - \varepsilon_n(\boldsymbol{k}))\, \mathrm{d}^m\boldsymbol{k} \tag{2}$$

where E is the energy for which the property has to be calculated, the summation is over the energy bands, V is the volume of the irreducible wedge (IW) of the first Brillouin zone, $f_n(\boldsymbol{k})$ is a property function for the nth band and $\varepsilon_n(\boldsymbol{k})$ is the dispersion relation for the nth band. If, for example, $f_n(\boldsymbol{k}) \equiv 1$, $I(E)$ is the density of states for the energy E: $D(E)$. $I(E)$ can be written as [1]

$$I(E) = \sum_n \int_{E=\varepsilon_n(\boldsymbol{k})} \frac{f_n(\boldsymbol{k})}{|\nabla\varepsilon_n(\boldsymbol{k})|}\, \mathrm{d}S \tag{3}$$

and is therefore also referred to as the 'surface integral'.

0022-3719/88/234263 + 21 $02.50

Figure 1. An example of the partitioning of an irreducible wedge (IW) (left) into a number of simplices (right) ($m = 2$).

The method commonly used to evaluate these integrals is the following. The IW can always be partitioned into a number of simplices (triangles in the two-dimensional case, tetrahedra in three dimensions) (figure 1). The $\boldsymbol{k}$-points for which the calculation is carried out are distributed over the simplices such that each simplex is partitioned into small ones (figure 2). The calculations are carried out in basic simplices, such as the ones indicated by shading in figure 2(b) and (c). Within each basic simplex i the functions $f_n(\boldsymbol{k})$ and $\varepsilon_n(\boldsymbol{k})$ are approximated by functions $f_{n,i}(\boldsymbol{k})$ and $\varepsilon_{n,i}(\boldsymbol{k})$ using the values of $f_n(\boldsymbol{k})$ and $\varepsilon_n(\boldsymbol{k})$ in the $\boldsymbol{k}$-points on the sides of the basic simplex. The basic simplices used in the calculation of $J(E)$ and $I(E)$ may be the smallest simplices with only $\boldsymbol{k}$-points at the corners (figure 2(b)), or larger simplices with additional $\boldsymbol{k}$-points on the sides (figure 2(c)). A simplex with only $\boldsymbol{k}$-points at the corners affords linear interpolation of $f_n(\boldsymbol{k})$ and $\varepsilon_n(\boldsymbol{k})$, but additional $\boldsymbol{k}$-points make it possible to obtain higher-order approximations. The integrals $J(E)$ and $I(E)$ become

$$J(E) = \sum_n \sum_i \int_{V_i} f_{n,i}(\boldsymbol{k})\theta(E - \varepsilon_{n,i}(\boldsymbol{k}))\, \mathrm{d}^m\boldsymbol{k} \equiv \sum_n \sum_i J_{n,i}(E) \tag{4}$$

and

$$I(E) = \sum_n \sum_i \int_{V_i} f_{n,i}(\boldsymbol{k})\delta(E - \varepsilon_{n,i}(\boldsymbol{k}))\, \mathrm{d}^m\boldsymbol{k} \equiv \sum_n \sum_i I_{n,i}(E) \tag{5}$$

where i is a sum over the basic simplices and V_i is the volume of the ith simplex. Given the orders of interpolation of $f_n(\boldsymbol{k})$ and $\varepsilon_n(\boldsymbol{k})$, the basic integrals $J_{n,i}(E)$ and $I_{n,i}(E)$ may in some cases be evaluated analytically. If not, additional approximations are introduced in the integral evaluation step. We may therefore classify BZ integration schemes according to the orders of interpolation of $f_n(\boldsymbol{k})$ and $\varepsilon_n(\boldsymbol{k})$ (usually but not necessarily the same), and the integral evaluation (analytic or approximate).

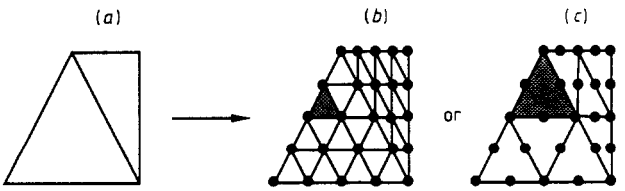

Figure 2. A possible distribution of $\boldsymbol{k}$-points over the simplices of an irreducible wedge (a) such that each simplex is partitioned into smaller ones. The basic simplices used in the calculations either have only $\boldsymbol{k}$-points at the corners (b) for linear methods, or have $\boldsymbol{k}$-points on the sides as well (c) for quadratic methods. In comparisons (§ 4) the same number of $\boldsymbol{k}$-points is used as in (b) and (c).

Of the various ways of interpolation, linear interpolation of both $f_n(\boldsymbol{k})$ and $\varepsilon_n(\boldsymbol{k})$ is by far the most popular, because it admits analytic evaluation of both $J_{n,i}(E)$ and $I_{n,i}(E)$ for $m = 3$ [2–6], for $m = 2$ [7, 8] and for $m = 1$. It suffers from some basic flaws, however, such as its behaviour for energies near Van Hove singularities [9]. Therefore quadratic interpolation of $f_n(\boldsymbol{k})$ and $\varepsilon_n(\boldsymbol{k})$ has been proposed [9]. For a long time, however, analytic evaluation of $J_{n,i}(E)$ and $I_{n,i}(E)$ with quadratic functions $f_{n,i}(\boldsymbol{k})$ and $\varepsilon_{n,i}(\boldsymbol{k})$ was only possible for $m = 1$. For $m = 2$ and $m = 3$ only approximate evaluation of $J_{n,i}(E)$ and $I_{n,i}(E)$ has been possible (for excellent reviews see Gilat [10] and Reser [11]; see also [12–14]). Although the results are usually reasonable for the various ways of integral approximation [10], this does not hold at energies near Van Hove singularities, where the convergence behaviour (oscillatory) and convergence rate (slow) are poor in contrast with those for an exact (analytic) evaluation of the integrals. An important contribution was therefore made by Methfessel *et al* [15], who succeeded in evaluating $I_{n,i}(E)$ analytically with for $\varepsilon_n(\boldsymbol{k})$ a second-order (quadratic) interpolation, and for $f_n(\boldsymbol{k})$ a zeroth-order [16] (i.e. $f_{n,i}(\boldsymbol{k}) = 1$, $I_{n,i}(E) = D_{n,i}(E)$) or first-order approximation [17] for the three-dimensional case ($m = 3$). Since their method is a geometrical one, it is difficult to extend it to $f_n(\boldsymbol{k})$ interpolated to quadratic order. However, much can be gained for the case of a general function $f_n(\boldsymbol{k})$ if a quadratic interpolation can also be treated, as we show in this paper for the two-dimensional case ($m = 2$).

We present here a new method for the analytic quadratic evaluation of the surface integral $I(E)$. The method is very different from the recent quadratic method of Methfessel and co-workers [15–17], in that it does not use projective geometry, but is algebraic in nature. The method is derived in detail for the two-dimensional case ($m = 2$). In essence, a transformation of variables is carried out in such a way that for a quadratic dispersion relation $\varepsilon_n(\boldsymbol{k})$ the surface integral (a line integral in the two-dimensional case) reduces to a one-dimensional integral, which can be evaluated analytically. We will demonstrate this for a quadratic function $f_n(\boldsymbol{k})$, but there are in fact no restrictions on the function $f_n(\boldsymbol{k})$ other than the requirement that the integrals exist. This is in fact the main advantage over the method of Methfessel and co-workers [15–17]. It will be shown that quadratic interpolation of $f_n(\boldsymbol{k})$ (in addition to $\varepsilon_n(\boldsymbol{k})$) is important for functions $f_n(\boldsymbol{k})$ which have similar oscillatory behaviour as $\varepsilon_n(\boldsymbol{k})$, and constitutes a major improvement indeed for functions which are more rapidly varying.

A brief outline of this paper is as follows: in § 2 we introduce our method and discuss the application of it to the frequently used linear approximation. The analytic quadratic evaluation of $I(E)$ is presented in § 3. In § 4 the performance of the method is shown by calculating tight-binding Brillouin zone integrals with the same number of $\boldsymbol{k}$-points for both methods. In the Appendices details of the derivations are given and a few related subjects are treated.

2. Linear interpolation

Let $f(x, y)$ and $\varepsilon(x, y)$ be of degree one:

$$f_1(x, y) = p_1 + p_2 x + p_3 y \tag{6a}$$

$$\varepsilon_1(x, y) = q_1 + q_2 x + q_3 y. \tag{6b}$$

The constants p_i and q_i can be found from the values of $f(x, y)$ and $\varepsilon(x, y)$ in the vertices of the triangle by solving two systems of three linear equations in three unknowns. The

integral $I(E)$ becomes

$$I(E) = \sum_{i=1}^{3} p_i V_i(E) \tag{7}$$

where (the explicit energy dependence of the integrals is dropped)

$$V_i = \int_V \mu_i(x, y)\delta(E - \varepsilon_1(x, y))\,\mathrm{d}x\,\mathrm{d}y \tag{8}$$

and $\mu_i(x, y) = 1, x, y$ for $i = 1, 2, 3$. So if it is possible to evaluate the integrals V_i, it is also possible to integrate any linear function $f_1(x, y)$. Note that $V_1(E)$ is the density of states at energy E: $D(E)$.

In order to evaluate integrals of the form

$$\int_V f(x, y)\delta(E - \varepsilon(x, y))\,\mathrm{d}x\,\mathrm{d}y \tag{9}$$

a transformation is made from the variables (x, y) to the variables (e, u):

$$x = g(e, u) \qquad y = h(e, u) \tag{10}$$

such that

$$\varepsilon(x, y) = \varepsilon(g(e, u), h(e, u)) = \varepsilon(e, u) \equiv e. \tag{11}$$

This transformation can be seen as a parametrisation of all surfaces $e = \varepsilon(x, y)$ in the parameter u. This transformation will therefore also be referred to as 'parametrisation'. The integral becomes

$$\int_{V_{e,u}} f(e, u)\delta(E - \varepsilon(e, u))\left[\frac{\partial(x, y)}{\partial(e, u)}\right]\mathrm{d}e\,\mathrm{d}u \tag{12}$$

where $V_{e,u}$ denotes the domain in e, u space corresponding to V in x, y space. This particular parametrisation removes the δ-function:

$$\int_{V_{e,u}} f(e, u)\delta(E - e)\left[\frac{\partial(x, y)}{\partial(e, u)}\right]\mathrm{d}e\,\mathrm{d}u = \int_{V_u(E)} f(E, u)\left[\frac{\partial(x, y)}{\partial(e, u)}\right]_{e=E}\mathrm{d}u. \tag{13}$$

This integral can only be non-zero of course if E lies within the range of the function $\varepsilon(x, y)$ over the triangle. It is also possible, although more cumbersome, to treat the surface integral form (3) of $I(E)$ with such a parametrisation (see Appendix 3).

When using linear interpolation, the surfaces $e = \varepsilon_1(x, y)$ are straight lines and the parametrisations are easily given. The corners of the triangle are numbered such that $\varepsilon_1 < \varepsilon_2 < \varepsilon_3$. Two cases have to be considered:

(i) $\varepsilon_1 < e < \varepsilon_2$ (figure 3):

$$\boldsymbol{k} = \boldsymbol{k}_1 + \frac{e - \varepsilon_1}{\varepsilon_3 - \varepsilon_1}(\boldsymbol{k}_3 - \boldsymbol{k}_1) + u\left[\frac{e - \varepsilon_1}{\varepsilon_2 - \varepsilon_1}(\boldsymbol{k}_2 - \boldsymbol{k}_1) - \frac{e - \varepsilon_1}{\varepsilon_3 - \varepsilon_1}(\boldsymbol{k}_3 - \boldsymbol{k}_1)\right] \tag{14}$$

where $0 \leqslant u \leqslant 1$. The Jacobian is

$$\left[\frac{\partial(x, y)}{\partial(e, u)}\right] = \frac{e - \varepsilon_1}{(\varepsilon_2 - \varepsilon_1)(\varepsilon_3 - \varepsilon_1)}\begin{bmatrix} k_{3x} - k_{1x} & k_{2x} - k_{1x} \\ k_{3y} - k_{1y} & k_{2y} - k_{1y} \end{bmatrix}. \tag{15}$$

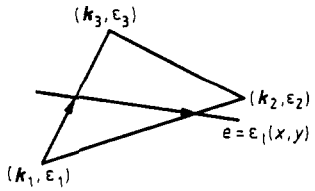

Figure 3. The vectors used for the parametrisation of the linear surface $e = \varepsilon_1(x, y)$ if $\varepsilon_1 < e < \varepsilon_2$.

The determinant is just twice the area of the triangle.

(ii) $\varepsilon_2 < e < \varepsilon_3$ (figure 4):

$$\boldsymbol{k} = \boldsymbol{k}_3 + \frac{e - \varepsilon_3}{\varepsilon_3 - \varepsilon_1}(\boldsymbol{k}_3 - \boldsymbol{k}_1) + u\left[\frac{e - \varepsilon_3}{\varepsilon_3 - \varepsilon_2}(\boldsymbol{k}_3 - \boldsymbol{k}_2) - \frac{e - \varepsilon_3}{\varepsilon_3 - \varepsilon_1}(\boldsymbol{k}_3 - \boldsymbol{k}_1)\right] \tag{16}$$

where $0 \leqslant u \leqslant 1$. The Jacobian is

$$\left[\frac{\partial(x, y)}{\partial(e, u)}\right] = \frac{\varepsilon_3 - e}{(\varepsilon_3 - \varepsilon_2)(\varepsilon_3 - \varepsilon_1)}\begin{bmatrix} k_{3x} - k_{2x} & k_{3x} - k_{1x} \\ k_{3y} - k_{2y} & k_{3y} - k_{1y} \end{bmatrix}. \tag{17}$$

The determinant is again twice the area of the triangle.

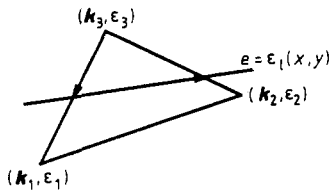

Figure 4. The vectors used for the parametrisation of the linear surface $e = \varepsilon_1(x, y)$ if $\varepsilon_2 < e < \varepsilon_3$.

In either case, the transformation is of the form

$$x = t_x(e) + uu_x(e) \qquad y = t_y(e) + uu_y(e) \qquad [\partial(x, y)/\partial(e, u)] = D(e) \tag{18}$$

where the Jacobian is denoted $D(e)$ as it will prove identical to the density of states. The integrals become

$$V_1 = \int_{V_{e,u}} \delta(E - e)D(e)\,\mathrm{d}e\,\mathrm{d}u = D(E)\int_0^1 \mathrm{d}u = D(E) \tag{19a}$$

$$V_2 = D(E)(t_x(E) + \tfrac{1}{2}u_x(E)) \tag{19b}$$

$$V_3 = D(E)(t_y(E) + \tfrac{1}{2}u_y(E)). \tag{19c}$$

3. Quadratic interpolation

Let the functions $f(x, y)$ and $\varepsilon(x, y)$ be of degree two

$$f_q(x, y) = p_1 + p_2x + p_3y + p_4x^2 + p_5xy + p_6y^2 \tag{20a}$$

$$\varepsilon_q(x, y) = q_1 + q_2x + q_3y + q_4x^2 + q_5xy + q_6y^2. \tag{20b}$$

The constants p_i and q_i can be found from the values of $f(x, y)$ and $\varepsilon(x, y)$ at the corners and the midpoints of the sides of the triangle by solving two systems of six linear equations in six unknowns. The integral $I(E)$ becomes

$$I(E) = \sum_{i=1}^{6} p_i V_i(E) \tag{21}$$

where (the explicit energy dependence of the integrals is dropped)

$$V_i = \int_V \mu_i(x, y)\delta(E - \varepsilon_q(x, y))\,\mathrm{d}x\,\mathrm{d}y \tag{22}$$

and $\mu_i(x, y) = 1, x, y, x^2, xy, y^2$ for $i = 1, 2, \ldots, 6$. So if it is possible to evaluate the integrals V_i, it is also possible to integrate any quadratic function $f_q(x, y)$. These integrals can be evaluated approximately by a variation on the so called 'hybrid method' [7]. The triangle is partitioned into as many smaller triangles as is desired. The energies at the corners of the smaller triangles are calculated using the quadratically interpolated $\varepsilon_q(x, y)$. Within the smaller triangles the integrals are evaluated using the linear interpolation for $\varepsilon_q(x, y)$ discussed in § 2. However, as we now have a quadratic $f_q(x, y)$ this requires in addition to the integrals V_1–V_3 for a linear $f_l(x, y)$ the evaluation of

$$V_i = \int_V \mu_i(x, y)\delta(E - \varepsilon_l(x, y))\,\mathrm{d}x\,\mathrm{d}y \tag{23}$$

and $\mu_i(x, y) = x^2, xy, y^2$ $(i = 4, 5, 6)$. Using the previously given parametrisation, these integrals become

$$V_4 = D(E)(t_x^2(E) + t_x(E)u_x(E) + \tfrac{1}{3}u_x^2(E)) \tag{24a}$$

$$V_5 = D(E)\{t_x(E)t_y(E) + \tfrac{1}{2}(t_x(E)u_y(E) + t_y(E)u_x(E)) + \tfrac{1}{3}u_x(E)u_y(E)\} \tag{24b}$$

$$V_6 = D(E)(t_y^2(E) + t_y(E)u_y(E) + \tfrac{1}{3}u_y^2(E)). \tag{24c}$$

This hybrid method will converge with increasing number of small triangles. It is desirable and possible, however, to evaluate the integrals fully analytically. For that purpose a parametrisation has to be found for $\varepsilon_q(x, y)$. Now it is well known that, apart from some degenerate cases, a quadratic surface represents either an ellipse, a hyperbola, a parabola or a straight line. It is not immediately evident for a general quadratic form which type of surface it represents. It is shown in Appendix 1 that there always exists an affine transformation:

$$\boldsymbol{k} = \mathbf{A}\boldsymbol{k}' + \boldsymbol{b} \tag{25}$$

which reduces the quadratic expression to a form from which the type of surface it represents can be inferred by inspection (table 1).

It should be noted that there is a certain freedom in the affine transformation. It is, for example, possible to reduce the forms further such that $|q_i| = 1$ for $i = 2, 3, \ldots, 6$. However, on the one hand it is desirable to limit the number of transformations as much as possible, because some of these transformations (such as translations and multiplications) might move the triangle far from the origin, which is likely to cause numerical problems. On the other hand one wants to reduce the quadratic surface as much as possible, because then the parametrisations and the evaluation of the integrals

Table 1. The various forms to which a quadratic surface may be reduced and the types of surfaces they represent. All constants $q_i (i = 2, 3, \ldots, 6)$ are essentially different from zero.

Reduced form	Surface
$\varepsilon_q(x, y) = q_1 + q_4 x^2 + q_6 y^2$ (q_4 and q_6 have equal signs)	Ellipse
$\varepsilon_q(x, y) = q_1 + q_5 xy$	Hyperbola
$\varepsilon_q(x, y) = q_1 + q_3 y + q_4 x^2$	Parabola
$\varepsilon_q(x, y) = q_1 + q_2 x$	Straight line
$\varepsilon_q(x, y) = q_1 + q_4 x^2$	Degenerate
$\varepsilon_q(x, y) = q_1$	Degenerate

are easy. The actual choice of the affine transformation has been determined by weighing these aspects against each other.

Parametrisations can be easily given for each of the reduced forms, as follows.

3.1. The ellipse

If $\varepsilon_q(x, y) = q_1 + q_4 x^2 + q_6 y^2$ (q_4 and q_6 have the same sign), the surfaces $e = \varepsilon_q(x, y)$ are ellipses with possible parametrisation

$$x = \{(e - q_1)/q_4\}^{1/2} \cos(u) \qquad y = \{(e - q_1)/q_6\}^{1/2} \sin(u) \tag{26}$$

where $0 \leqslant u < 2\pi$. The Jacobian is

$$[\partial(e, u)/\partial(x, y)] = 1/2(q_4 q_6)^{1/2}. \tag{27}$$

The integrals become (the limits on the u-integration are omitted, they will be specified later):

$$V_1 = \int_{V_{e,u}} \delta(E - e) \frac{1}{2(q_4 q_6)^{1/2}} \, de \, du = \frac{1}{2(q_4 q_6)^{1/2}} [u] \tag{28a}$$

$$V_2 = \{1/2(q_4 q_6)^{1/2}\}\{(E - q_1)/q_4\}^{1/2}[\sin(u)] \tag{28b}$$

$$V_3 = \{1/2(q_4 q_6)^{1/2}\}\{(E - q_1)/q_6\}^{1/2}[-\cos(u)] \tag{28c}$$

$$V_4 = \{1/2(q_4 q_6)^{1/2}\}\{(E - q_1)/q_4\}[\tfrac{1}{2}u + \tfrac{1}{4}\sin(2u)] \tag{28d}$$

$$V_5 = \{1/2(q_4 q_6)^{1/2}\}\{(E - q_1)/q_4\}^{1/2}\{(E - q_1)/q_6\}^{1/2}[-\tfrac{1}{4}\cos(2u)] \tag{28e}$$

$$V_6 = \{1/2(q_4 q_6)^{1/2}\}\{(E - q_1)/q_6\}[\tfrac{1}{2}u - \tfrac{1}{4}\sin(2u)]. \tag{28f}$$

3.2. The hyperbola

If $\varepsilon_q(x, y) = q_1 + q_5 xy$, the surfaces $e = \varepsilon_q(x, y)$ are hyperbolae with possible parametrisation

$$x = u \qquad y = (e - q_1)/q_5 u \tag{29}$$

where $-\infty < u < 0$ or $0 < u < \infty$. The Jacobian is

$$[\partial(x, y)/\partial(e, u)] = 1/|q_5 u|. \tag{30}$$

The integrals become

$$V_1 = \int_{V_{e,u}} \delta(E-e)\frac{\pm}{|q_5|u}\,\mathrm{d}u = \frac{\pm}{|q_5|}[\ln(u)] \tag{31a}$$

$$V_2 = \pm(1/|q_5|)[u] \tag{31b}$$

$$V_3 = \pm(1/|q_5|)\{(E-q_1)/q_5\}[-1/u] \tag{31c}$$

$$V_4 = \pm(1/|q_5|)[\tfrac{1}{2}u^2] \tag{31d}$$

$$V_5 = \pm(1/|q_5|)\{(E-q_1)/q_5\}[\ln(u)] \tag{31e}$$

$$V_6 = \pm(1/|q_5|)\{(E-q_1)^2/q_5^2\}[-1/2u^2]. \tag{31f}$$

3.3. The parabola

If $\varepsilon_q(x,y) = q_1 + q_3y + q_4x^2$, the surfaces $e = \varepsilon_q(x,y)$ are parabolae with possible parametrisation

$$x = u \qquad y = \{(e-q_1)/q_3\} - (q_4/q_3)u^2 \tag{32}$$

where $-\infty < u < \infty$. The Jacobian is

$$[\partial(x,y)/\partial(e,u)] = 1/|q_3|. \tag{33}$$

The integrals become

$$V_1 = \int_{V_{e,u}} \delta(E-e)\frac{1}{|q_3|}\,\mathrm{d}e\,\mathrm{d}u = \frac{1}{|q_3|}[u] \tag{34a}$$

$$V_2 = (1/|q_3|)[\tfrac{1}{2}u^2] \tag{34b}$$

$$V_3 = (1/|q_3|)[\{(E-q_1)/q_3\}u - \tfrac{1}{3}(q_4/q_3)u^3] \tag{34c}$$

$$V_4 = (1/|q_3|)[\tfrac{1}{3}u^3] \tag{34d}$$

$$V_5 = (1/|q_3|)[\tfrac{1}{2}\{(E-q_1)/q_3\}u^2 - \tfrac{1}{4}(q_4/q_3)u^4] \tag{34e}$$

$$V_6 = \frac{1}{|q_3|}\left[\frac{(E-q_1)^2}{q_3^2}u - \frac{2}{3}\frac{E-q_1}{q_3}\frac{q_4}{q_3}u^3 + \frac{1}{5}\frac{q_4^2}{q_3^2}u^5\right]. \tag{34f}$$

3.4. The straight line

If $\varepsilon_q(x,y) = q_1 + q_2x$, the surfaces $e = \varepsilon_q(x,y)$ are straight lines with possible parametrisation

$$x = (e-q_1)/q_2 \qquad y = u \tag{35}$$

where $-\infty < u < \infty$. The Jacobian is

$$[\partial(x,y)/\partial(e,u)] = 1/|q_2|. \tag{36}$$

The integrals become

$$V_1 = \int_{V_{e,u}} \delta(E-e)\frac{1}{|q_2|}\,\mathrm{d}e\,\mathrm{d}u = \frac{1}{|q_2|}[u] \tag{37a}$$

$$V_2 = (1/|q_2|)\{(E - q_1)/q_2\}[u] \tag{37b}$$

$$V_3 = (1/|q_2|)[\tfrac{1}{2}u^2] \tag{37c}$$

$$V_4 = (1/|q_2|)\{(E - q_1)^2/q_2^2\}[u] \tag{37d}$$

$$V_5 = (1/|q_2|)\{(E - q_1)/q_2\}[\tfrac{1}{2}u^2] \tag{37e}$$

$$V_6 = (1/|q_2|)[\tfrac{1}{3}u^3]. \tag{37f}$$

3.5. The degenerate form

If $\varepsilon_q(x, y) = q_1 + q_4x^2$ the surfaces $e = \varepsilon_q(x, y)$ consists of two parallel straight lines:

$$x = \pm\{(e - q_1)/q_4\}^{1/2} \tag{38}$$

with possible parametrisation:

$$x = \pm(e - q_1)/\{q_4(e - q_1)\}^{1/2} \qquad y = u \tag{39}$$

where $-\infty < u < \infty$. The Jacobian is:

$$[\partial(x, y)/\partial(e, u)] = 1/2\{q_4(e - q_1)\}^{1/2}. \tag{40}$$

Comparison of (39) and (40) with (35) and (36) shows that the integrals are the same as for the straight lines, divided by two. If $\varepsilon_q(x, y) = q_1$ the surface integrals are delta functions and cannot be specified.

The limits on the u-integration are also needed to evaluate the integrals. Firstly, the parameters specifying the points of intersection of the surface $E = \varepsilon_q(x, y)$ with the sides of the triangle are to be found. Let the sides of the triangle be given by

$$n_{jx}x + n_{jy}y = c_j \qquad (j = 1, 2, 3) \tag{41}$$

where $\boldsymbol{n}_j$ is a vector normal to side j of the triangle. If the surface $E = \varepsilon_q(x, y)$ is an ellipse, this requires the solution of the goniometric equations:

$$n_{jx}\{(E - q_1)/q_4\}^{1/2}\cos(u) + n_{jy}\{(E - q_1)/q_6\}^{1/2}\sin(u) = c_j \qquad (j = 1, 2, 3). \tag{42}$$

If the surface $E = \varepsilon_q(x, y)$ is a hyperbola this requires the solution of the quadratic equations:

$$n_{jx}u^2 - c_ju + n_{jy}\{(E - q_1)/q_5\} = 0 \qquad (j = 1, 2, 3). \tag{43}$$

If the surface $E = \varepsilon_q(x, y)$ is a parabola this requires the solution of the quadratic equations:

$$-n_{jy}(q_4/q_3)u^2 + n_{jx}u + n_{jy}\{(E - q_1)/q_3\} - c_j = 0 \qquad (j = 1, 2, 3). \tag{44}$$

If the surface $E = \varepsilon_q(x, y)$ is a straight line this requires the solution of the linear equations:

$$n_{jy}u + n_{jx}\{(E - q_1)/q_2\} - c_j = 0 \qquad (j = 1, 2, 3). \tag{45}$$

Secondly, the parameter values u_i corresponding to points of intersection are ordered. Points specified by consecutive parameters in this ordered list are connected because of the continuity of the parametrisations [18] (figure 5).

Finally, two consecutive parameters are averaged and the position relative to the triangle of the point specified by the averaged parameter is determined. (All that can be said of the position of this point relative to the two consecutive points is that it lies

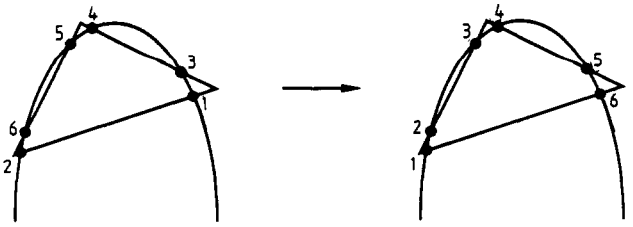

Figure 5. An example of the ordering of the parameters to find out which points specified by the parameters are connected. On the left, the parameters are numbered according to the order in which they are generated. On the right, the parameters are ordered in ascending order.

somewhere on the curve betweer them. It does not necessarily lie 'half way', because the parameter u is generally not equal to the arc length [18].) If it lies inside the triangle, the limits on the u-integration are those two consecutive parameters. Note that if the surface $E = \varepsilon_q(x, y)$ is an ellipse, an additional check is needed to determine whether the highest and the lowest parameters provide an additional integration domain (figure 6(a)). Furthermore, if there are no points of intersection, a check is needed to determine whether the ellipse lies entirely within the triangle. If so, the limits on the u-integration are 0 and 2π (figure 6(b)). If the surface $E = \varepsilon_q(x, y)$ is a hyperbola, two consecutive

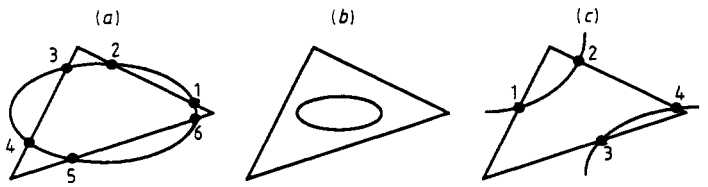

Figure 6. Illustrations of some special cases. (a) The points on the ellipse specified by the parameters 1 and 6 are connected, though the parameters are not consecutive. (b) The integration parameters are 0 and 2π, though there are no points of intersection of the ellipse with the triangle. (c) The points of the hyperbola specified by the parameters 2 and 3 are not connected, though they are consecutive.

parameters which have opposite signs may not be averaged, for they are not connected (figure 6(c)). The integrals V' thus obtained are integrals over the transformed quadratic surface and must be transformed back in order to obtain the values of the integrals V over the original surface. If the affine transformation is

$$\begin{aligned} x &= a_{11}x' + a_{12}y' + b_1 \\ y &= a_{21}x' + a_{22}y' + b_2 \\ [\partial(x, y)/\partial(x', y')] &= |a_{11}a_{22} - a_{12}a_{21}| = 1 \end{aligned} \tag{46}$$

(see Appendix 1) then

$$V_1 = \int_V \delta(E - \varepsilon_q(x, y))\,\mathrm{d}x\,\mathrm{d}y = \int_V \delta(E - \varepsilon_q'(x', y'))\,\mathrm{d}x'\,\mathrm{d}y' = V_1' \tag{47a}$$

$$V_2 = a_{11}V_2' + a_{12}V_3' + b_1V_1' \tag{47b}$$

$$V_3 = a_{21}V_2' + a_{22}V_3' + b_2V_1' \tag{47c}$$

$$V_4 = a_{11}^2V_4' + a_{12}^2V_6' + b_1^2V_1' + 2(a_{11}a_{12}V_5' + a_{11}b_1V_2' + a_{12}b_1V_3') \tag{47d}$$

$$V_5 = a_{11}a_{21}V_4' + a_{12}a_{22}V_6' + b_1b_2V_1' + (a_{11}a_{22} + a_{21}a_{12})V_5' + (a_{11}b_2 + a_{21}b_1)V_2' + (a_{12}b_2 + a_{22}b_1)V_3' \tag{47e}$$

$$V_6 = a_{21}^2V_4' + a_{22}^2V_6' + b_2^2V_1' + 2(a_{21}a_{22}V_5' + a_{21}b_2V_2' + a_{22}b_2V_3'). \tag{47f}$$

Our presentation thus far suggests that it is necessary for the evaluation of $I(E)$ to determine for each triangle and each function $f(x, y)$ the expansion coefficients p_i. This is not the case. As this is a matter of great practical utility we discuss it in some detail in Appendix 2.

4. Performance of the method

The performance of the method is tested by calculating the tight-binding density of states (the usual test case in the literature [11]):

$$\int_{-1}^{1}\int_{-1}^{1} \delta\{E + \tfrac{1}{2}(\cos(\pi x) + \cos(\pi y))\}\,\mathrm{d}x\,\mathrm{d}y \tag{48}$$

and the tight-binding Green function integrals (the test cases proposed by Methfessel *et al* [17]):

$$\int_{-1}^{1}\int_{-1}^{1} (\cos(n\pi x) + \cos(n\pi y))\delta\{E + \tfrac{1}{2}(\cos(\pi x) + \cos(\pi y))\}\,\mathrm{d}x\,\mathrm{d}y \tag{49}$$

for $n = 1$, 3 and 6 by:

(i) constant (least-squares) approximation of $f(x, y)$ and linear interpolation of $\varepsilon(x, y)$ (abbreviated as cl) (sometimes used, Chen [13])

(ii) linear interpolation of both $f(x, y)$ and $\varepsilon(x, y)$ (ll) (commonly used, Lehmann and Taut [4])

(iii) linear (least-squares) approximation of $f(x, y)$ and quadratic interpolation of $\varepsilon(x, y)$ (lq) (proposed by Methfessel *et al* [17])

(iv) quadratic interpolation of both $f(x, y)$ and $\varepsilon(x, y)$ (qq) (proposed here)

for an increasing number of $\boldsymbol{k}$-points along the edges of the IW (denoted by N; the total number of $\boldsymbol{k}$-points is $N(N + 1)/2$.

The calculations were carried out for 400 evenly spaced energies in the range $[-1, +1]$ and the root-mean-square deviation (denoted by RMS) from the exact (converged) result was determined. All methods used the same number of $\boldsymbol{k}$-points, which was accomplished by a division of the triangles in which the (lq) and (qq) integration were carried out into four smaller triangles in which the (cl) and (ll) integration were performed (see figure 2). As suggested by Jansen and Freeman [19], the logarithm of RMS is plotted against the logarithm of N.

N must of course be large enough to resolve the oscillations in the functions $\varepsilon(x, y)$ and $f(x, y)$. A reasonable minimum seems one plus the number of extrema of these functions along an edge of the IW.

Considering first figure 7(*a*) with $f(x, y) = 1$ (the density of states), the curves for (cl) and (ll) coincide, as do those for (lq) and (qq), because the approximation for $f(x, y)$ (c, l or q) is irrelevant for constant $f(x, y)$. Figure 7(*a*) clearly demonstrates the superiority of the quadratic approximation to $\varepsilon(x, y)$, in agreement with the findings of Boon *et al* [16]. (All of the methods happen to coincide in figure 7(*a*) when N equals 3, because then the quadratically interpolated $\varepsilon_q(x, y)$ is accidentally linear.) Considering next the case with $f(x, y) = \cos(\pi x) + \cos(\pi y)$ (figure 7(*b*)), we note that the (qq) method is superior, as expected. The (lq) method, although inferior to (qq), represents a distinct improvement over the standard linear method (ll), and of course over (cl). This changes when the function $f(x, y)$ becomes more rapidly varying (figures 7(*c*) and (*d*)). In these cases the superior performance of the (qq) method is particularly striking. It is surprising at first sight that the (lq) method is doing so poorly, being in figure 7(*d*) even inferior to (ll) for the N-values shown. This is due to the fact that the (lq) method, for consistency with the approach of Methfessel *et al* [17], uses a linear least-squares approximation of $f(x, y)$ in the *large* triangles, which have ***k***-points at the corners and the midpoints of the edges, whereas the (ll) method uses a separate linear interpolation in each of the four smaller triangles into which the large triangle may be subdivided (see figure 2). Apparently the advantage of a finer division of the IW in the (ll) method, for the same ***k***-point density, outweighs the advantage of the quadratic interpolation of $\varepsilon(x, y)$ in the (lq) method. (The phenomenon of different methods giving an identical log(RMS) at

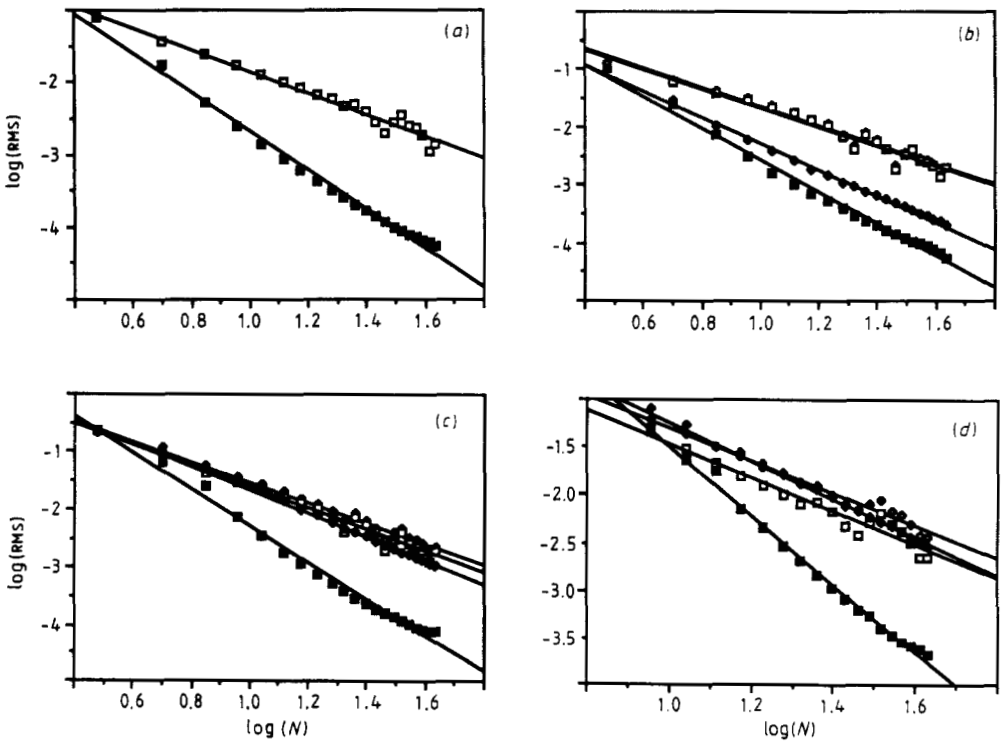

Figure 7. Convergence behaviour of different ways to evaluate the integrals: ◇, cl; □, ll; ◆, lq; ■, qq. The converged result was a (qq) calculation with $N = 243$. (*a*) $f(x, y) = 1$. (*b*) $f(x, y) = \cos(\pi x) + \cos(\pi y)$. (*c*) $f(x, y) = \cos(3\pi x) + \cos(3\pi y)$ and (*d*) $f(x, y) = \cos(6\pi x) + \cos(6\pi y)$.

particular values of N, due to accidental linear behaviour of the quadratic interpolation, occurs in each case: in figure 7(*b*) (ll), (lq) and (qq) coincide at $N = 3$ because both $f(x, y)$ and $\varepsilon(x, y)$ are linear; in figure 7(*c*) (lq) and (qq) coincide at $N = 9$, because $f((x, y)$ is linear; in figure 7(*d*) this happens at $N = 13$.)

The general conclusion is that the (qq) integration shows considerably better convergence characteristics than all other methods. The difference with the other methods is particularly striking when the function $f(x, y)$ is rapidly varying (figure 7(*d*)). This may be analysed more quantitatively. The almost linear dependence of log(RMS) on log(N) implies that the error behaves as:

$$\text{RMS}(N) = \alpha N^{-\beta} \tag{50}$$

where α and β are positive constants. It is interesting to compare the exponents β for the different ways to evaluate the various integrals, since these directly reflect the convergence rate (table 2). Roughly, the exponents β are twice as large for the analytic quadratic integration as for the analytic linear integration. So, to achieve the same accuracy with quadratic integration as with linear integration, in the limit of large N only about the square root of the total number of $\boldsymbol{k}$-points is needed. This is not quite true for the density of states (column (*a*)), but it definitely is for rapidly varying $f(x, y)$ (column (*d*)). In the latter case as well as in case (*c*), the major improvement occurs in going to (qq). The advantage will be less favourable near band crossings of course, but there is no reason to assume that the quadratic integration will be worse than the linear in such cases.

Table 2. Comparison of the exponentials β in equation (50) for different ways to evaluate various integrals. (*a*), (*b*), (*c*) and (*d*) are as in figure 7.

	(*a*)	(*b*)	(*c*)	(*d*)
(cl)	1.5	1.7	1.8	1.7
(ll)	1.5	1.7	1.8	1.7
(lq)	2.7	2.3	2.0	2.0
(qq)	2.7	2.8	3.2	3.6

5. Summary and conclusions

A method for analytic quadratic integration over the two-dimensional Brillouin zone has been presented. Quadratic approximations were used for both the dispersion relation $\varepsilon(x, y)$ and the property function $f(x, y)$. We have shown that convergence rate and convergence behaviour are far better for the analytic quadratic integration than those for the commonly used analytic linear integration. The improvement is particularly striking when $f(x, y)$ exhibits significant variation over the Brillouin zone. Roughly, analytic quadratic integration can achieve the same accuracy as analytic linear integration with only about the square root of the total number of $\boldsymbol{k}$-points needed. A software package (in FORTRAN) is available on request.

The considerable saving in computation time achieved here for the two-dimensional case is important for the relatively time-consuming slab calculations it was originally developed for. The method can in principle be extended to the three-dimensional case. The surface integral then reduces to an integral over two variables that parametrise the

energy surface. The quadratic surfaces can be grouped into nine classes. The analytic quadratic evaluation of the integrals has been solved for six of these classes. Research is still going on for the remaining three classes.

Appendix 1. Construction of the affine transformation

There always exists an affine transformation $\boldsymbol{k} = \mathbf{A}\boldsymbol{k}' + \boldsymbol{b}$ which reduces a general quadratic surface to a form from which the type of surface it represents can be inferred by inspection. The affine transformation will be explicitly constructed here, proving the existence of the affine transformation, and at the same time providing a suitable algorithm for its construction. Consider a general quadratic form:

$$\varepsilon_q(x, y) = q_1 + q_2x + q_3y + q_4x^2 + q_5xy + q_6y^2. \tag{A1.1}$$

If $q_5 \neq 0$ there exists a transformation $\boldsymbol{k} = \mathbf{A}\boldsymbol{k}'$ with $|\det(\mathbf{A})| = 1 = 1$ such that $q_5 = 0$. This is easily seen if $\varepsilon_q(x, y)$ is rewritten as

$$\varepsilon_q(x, y) = r + \boldsymbol{k}^T\boldsymbol{t} + \boldsymbol{k}^T\mathbf{S}\boldsymbol{k} \tag{A1.2}$$

where

$$r = q_1 \qquad \boldsymbol{t} = \begin{pmatrix} q_2 \\ q_3 \end{pmatrix} \qquad \mathbf{S} = \tfrac{1}{2}\begin{pmatrix} 2q_4 & q_5 \\ q_5 & 2q_6 \end{pmatrix}. \tag{A1.3}$$

Application of the transformation $\boldsymbol{k} = \mathbf{A}\boldsymbol{k}'$ yields

$$\varepsilon'_q(x', y') = r + \boldsymbol{k}'^T(\mathbf{A}^T\boldsymbol{t}) + \boldsymbol{k}'^T(\mathbf{A}^T\mathbf{S}\mathbf{A})\boldsymbol{k}'. \tag{A1.4}$$

$\mathbf{A}$ is thus the matrix which diagonalises $\mathbf{S}$.

$\varepsilon'_q(x', y')$ is now of the form

$$\varepsilon_q(x, y) = q_1 + q_2x + q_3y + q_4x^2 + q_6y^2. \tag{A1.5}$$

If $q_4 = 0$ and $q_6 \neq 0$ there exists a transformation $\boldsymbol{k} = \mathbf{A}\boldsymbol{k}'$ with $|\det(\mathbf{A})| = 1$ such that $q'_4 \neq 0$ and $q'_6 = 0$:

$$x = y' \qquad y = x'. \tag{A1.6}$$

If $q_4 \neq 0$ and $q_2 \neq 0$ there exists a transformation $\boldsymbol{k} = \boldsymbol{k}' + \boldsymbol{b}$ such that $q'_2 = 0$:

$$x = x' - q_2/2q_4 \qquad y = y' \tag{A1.7}$$

$$\begin{aligned}\varepsilon'_q(x', y') &= q_1 + q_2(x' - q_2/2q_4) + q_3y' + q_4(x' - q_2/2q_4)^2 + q_6y'^2 \\ &= q_1 - q_2^2/4q_4 + q_3y' + q_4x'^2 + q_6y'^2.\end{aligned} \tag{A1.8}$$

Likewise, if $q_6 \neq 0$ and $q_3 \neq 0$ there exists a transformation $\boldsymbol{k} = \boldsymbol{k}' + \boldsymbol{b}$ such that $q'_3 = 0$:

$$x = x' \qquad y = y' - q_3/2q_6. \tag{A1.9}$$

With these transformations $\varepsilon_q(x, y)$ is reduced to one of the following forms:

$$\varepsilon_q(x, y) = q_1 + q_4x^2 + q_6y^2 \qquad (q_4 \neq 0 \text{ and } q_6 \neq 0) \tag{A1.10a}$$

$$\varepsilon_q(x, y) = q_1 + q_3y + q_4x^2 \qquad (q_4 \neq 0,\ q_3 \text{ may be } 0) \tag{A1.10b}$$

$$\varepsilon_q(x, y) = q_1 + q_2x + q_3y \qquad (q_2 \text{ and (or) } q_3 \text{ may be } 0). \tag{A1.10c}$$

If $\varepsilon_q(x, y) = q_1 + q_4x^2 + q_6y^2$ ($q_4 \neq 0$ and $q_6 \neq 0$) and q_4 and q_6 have *the same* sign, the surfaces $e = \varepsilon_q(x, y)$ are ellipses.

If $\varepsilon_q(x, y) = q_1 + q_4x^2 + q_6y^2$ ($q_4 \neq 0$ and $q_6 \neq 0$) and q_4 and q_6 have *opposite* signs, the surfaces $e = \varepsilon_q(x, y)$ are hyperbolae. For ease of parametrisation, it is further reduced by a transformation $\boldsymbol{k} = \mathbf{A}\boldsymbol{k}'$ with $|\det(\mathbf{A})| = 1$ such that $q_4' = 0$, $q_6' = 0$ and $q_5' \neq 0$:

$$x = x'/(\sqrt{2}) + (|q_6/|2q_4|)^{1/2}y' \qquad y = (|q_4|/|2q_6|)^{1/2}x' - y'(\sqrt{2}) \tag{A1.11}$$

$$\begin{aligned}\varepsilon_q'(x', y') &= q_1 + q_4\{x'/(\sqrt{2}) + (|q_6|/|2q_4|)^{1/2}y'\}^2 + q_6\{(|q_4|/|2q_6|)^{1/2}x' - y'/(\sqrt{2})\}^2 \\ &= q_1 + \tfrac{1}{2}\{q_4 + q_6(|q_4|/|q_6|)\}x'^2 + \{q_4(|q_6|/|q_4|)^{1/2} - q_6(q_4/q_6)^{1/2}\}x'y' \\ &\quad + \tfrac{1}{2}\{q_4|q_6|/|q_4| + q_6\}y'^2 \\ &= q_1' + q_4'x'^2 + q_5'x'y' + q_6'y'^2. \end{aligned} \tag{A1.12}$$

Now $q_4' = 0$, $q_6' = 0$ and $q_5' \neq 0$ because q_4 and q_6 have the same sign.

If $\varepsilon_q(x, y) = q_1 + q_3y + q_4x^2$ ($q_3 \neq 0$ and $q_4 \neq 0$) the surfaces $e = \varepsilon_q(x, y)$ are parabolae.

If $\varepsilon_q(x, y) = q_1 + q_4x^2$ ($q_4 \neq 0$) the surfaces $e = \varepsilon_q(x, y)$ consist of two parallel straight lines.

If $\varepsilon_q(x, y) = q_1 + q_2x + q_3y$ ($q_2 \neq 0$ and (or) $q_3 \neq 0$) the surfaces $e = \varepsilon_q(x, y)$ are straight lines. To treat one of the degenerate cases as two straight lines, it is further reduced by a transformation $\boldsymbol{k} = \mathbf{A}\boldsymbol{k}'$ with $|\det(\mathbf{A})| = 1$ such that $q_2' \neq 0$ and $q_3' = 0$:

$$\begin{aligned} &x = x'\cos\theta + y'\sin\theta \qquad y = x'\sin\theta - y'\cos\theta \\ &\cos\theta = q_2/(q_2^2 + q_3^2)^{1/2} \\ &\sin\theta = q_3/(q_2^2 + q_3^2)^{1/2}. \end{aligned} \tag{A1.13}$$

$\varepsilon_q'(x', y')$ is now of the form (primes dropped)

$$\varepsilon_q(x, y) = q_1 + q_2x. \tag{A1.14}$$

Appendix 2. Integrals over the Brillouin zone

A2.1. General procedure

We will demonstrate in this Appendix that the integral $I(E)$ can be cast in the convenient form

$$I(E) = \sum_{j=1}^{n} w_j(E) f(\boldsymbol{k}_j) \tag{A2.1}$$

where the $f(\boldsymbol{k}_j)$ are the values of $f(\boldsymbol{k})$ at the $\boldsymbol{k}$-points of the simplex under consideration and the $w_j(E)$ are constants independent of $f(\boldsymbol{k})$ and independent of the shape of the simplex. They do depend of course on the dispersion relation $\varepsilon(\boldsymbol{k})$. With a suitable redefinition of the $w_j(E)$ an exactly similar expression holds for the volume integral $J(E)$. The argument is general, but we will give it for the specific case of two dimensions (the simplex is a triangle) and quadratic interpolation ($n = 6$).

In this paper we used the fact that when the $V_i(E)$, $i = 1, 2, \ldots, 6$ defined as the integrals $I_{\mu i}(E)$ of the monomials $\mu_i = 1, x, y, x^2, xy$ and y^2 are known, we can compute

the integral of any function $f(\boldsymbol{k})$ approximated by a second-degree polynomial. Let the expansion of $f(\boldsymbol{k})$ be

$$f(\boldsymbol{k}) = \sum_{i=1}^{6} p_i \mu_i(\boldsymbol{k}) \tag{A2.2}$$

then

$$I_f(E) = \sum_{i=1}^{6} p_i I_{\mu_i}(E) = \sum_{i=1}^{6} p_i V_i(E). \tag{A2.3}$$

The expansion coefficients p_i can be calculated if the values $f(\boldsymbol{k}_j)$ are known in the vertices and midpoints of the edges. This requires the solution of a linear system of six equations in six unknowns:

$$\sum_{j=1}^{6} \mu_j(\boldsymbol{k}_i) p_j = f(\boldsymbol{k}_i) \qquad (i = 1, 2, \ldots, 6). \tag{A2.4}$$

The p_j depend on $f(\boldsymbol{k})$, so it appears at first sight that we have to construct the expansion coefficients for each particular $f(\boldsymbol{k})$ in order to compute the integral by (A2.3). It is easily shown however that this is not necessary. The argument is not specific for the integrals $I(E)$ and $J(E)$, but holds generally for any linear functional L defined on a class of function f which may be expanded in a complete and independent basis set, e.g. $\{\mu_i; i = 1, 2, \ldots, n\}$. Let the values $L[\mu_i]$, $i = 1, 2, \ldots, n$ be known (cf. our $V_i(E)$), and let n points $\boldsymbol{k}_j$ be given in which the function values $f(\boldsymbol{k}_j)$ can be calculated. The expansion coefficients p_i are defined if the matrix $\mathbf{F}$, $F_{ji} \equiv \mu_i(\boldsymbol{k}_j)$ is non-singular:

$$p_i = \sum_{j=1}^{n} F_{ij}^{-1} f(\boldsymbol{k}_j) \qquad (i = 1, 2, \ldots, n). \tag{A2.5}$$

The expression for $L[f]$ becomes

$$\begin{aligned} L[f] = L \sum_{i=1}^{n} p_i \mu_i &= \sum_{i=1}^{n} \sum_{j=1}^{n} F_{ij}^{-1} f(\boldsymbol{k}_j) L[\mu_i] \\ &= \sum_{j=1}^{n} \left(\sum_{i=1}^{n} F_{ij}^{-1} L[\mu_i] \right) f(\boldsymbol{k}_j) \equiv \sum_{j=1}^{n} w_j f(\boldsymbol{k}_j) \end{aligned} \tag{A2.6}$$

with

$$w_j = \sum_{i=1}^{n} F_{ij}^{-1} L[\mu_i] \qquad (j = 1, 2, \ldots, n). \tag{A2.7}$$

Equation (A2.7) shows that the weights w_j are independent of the function $f_n(\boldsymbol{k})$. We will show that they are also independent of the shape of the simplex, apart from a numerical constant which is equal to twice the area of the simplex.

Equation (A2.6) (see also (A2.1)) is in fact a numerical integration formula with n nodes $\boldsymbol{k}_j$ and n weights w_j. In our case (quadratic interpolation ($n = 6$)) the formula is of degree 2, i.e. it is exact for polynomials of degree 2 or less. The integration region is a triangle and the weight function is either the δ-function or the θ-function for I and J respectively. So it is possible to make a final simplification using the standard theory of numerical integration. Under a transformation of variables, which maps the region of

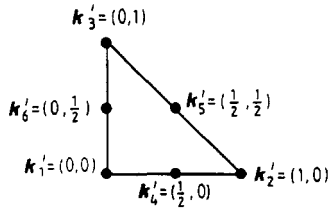

Figure A1. The standard triangle.

integration R into the region R', we obtain the nodes of an integration formula for R' by applying the transformation to the nodes of the formula for R. For an affine transformation, $\boldsymbol{k}' = \mathbf{A}\boldsymbol{k} + \boldsymbol{b}$, the resulting formula has the same degree of accuracy as the old one and the new weights w'_j are the old weights multiplied by the determinant of the transformation [20]. Since there always exists an affine transformation which maps a particular triangle onto the standard triangle of figure A1 (all triangles are affine to each other), the weights w_j can be evaluated using this triangle.

For this triangle the matrices $\mathbf{F}$ and $\mathbf{F}^{-1}$ are very simple. In particular we have

$$\mathbf{F}^{-1} = \begin{pmatrix} 1 & 0 & 0 & 0 & 0 & 0 \\ -3 & -1 & 0 & 4 & 0 & 0 \\ -3 & 0 & -1 & 0 & 0 & 4 \\ 2 & 2 & 0 & -4 & 0 & 0 \\ 4 & 0 & 0 & -4 & 4 & -4 \\ 2 & 0 & 2 & 0 & 0 & -4 \end{pmatrix}. \tag{A2.8}$$

Now the weights w'_j are easily found in terms of the V'_i using this matrix and relation (A2.7). To evaluate the V'_i we need the (tranformed) dispersion relation $\varepsilon'_n(\boldsymbol{k}')$ in the standard triangle. This is trivial as $\varepsilon'_n(\boldsymbol{k}'_j) = \varepsilon_n(\boldsymbol{k}_j)$. The coefficients of the quadratic expansion are determined as $q_i = \Sigma F^{-1}_{ij} \varepsilon'_n(\boldsymbol{k}'_j)$ and, again, matrix $\mathbf{F}^{-1}$ is given by (A2.8). Finally, to obtain the weights w_j in the original coordinate frame we only have to multiply the w'_j by the determinant of the affine transformation, which is equal to twice the area of the actual triangle.

A2.2. Volume integrals

We wish to make a few remarks concerning the computation of the volume integrals

$$J(E) = \int f(\boldsymbol{k})\theta(E - \varepsilon(\boldsymbol{k}))\,\mathrm{d}\boldsymbol{k} \tag{A2.9}$$

with $f(\boldsymbol{k})$ and $\varepsilon(\boldsymbol{k})$ approximated by quadratic functions. These are frequently needed, for example to obtain the charge density of a crystal from the eigenstates of the Hamiltonian, known in some points of the Brillouin zone. In that case $f(\boldsymbol{k})$ is the charge density corresponding to the eigenstates in $\boldsymbol{k}$.

Following the procedure outlined in §A2.1 we can numerically approximate any type of integral of a function $f(\boldsymbol{k})$, provided we have the values of V_i, i.e. the analogous integrals of the monomials μ_i. The weights w_j of the numerical integration formula are fixed linear combinations of the V_i.

As mentioned before we may assume that the region of integration, a triangle, is some standard triangle. The formulae for the V_i have been given in this paper for the case of the surface integrals:

$$I_\mu(E) = \int \mu(\boldsymbol{k})\delta(E - \varepsilon(\boldsymbol{k}))\,\mathrm{d}\boldsymbol{k}. \tag{A2.10}$$

We have not been able, however, to derive all necessary analytical expressions for the volume integrals (A2.9).

Clearly, if the energy surface, defined by $\varepsilon(\boldsymbol{k}) = E$, has no points inside the triangle, then the function $\theta(E - \varepsilon(\boldsymbol{k}))$ is either zero or one in the whole region. In the former case all V_i are zero. In the latter case the V_i are easily calculated; the weights following from them (equations (A2.7) and (A2.8)) are remarkable: those corresponding to the three vertices are zero, while the other three are equal to one third of the area of the triangle each. This means that for isolators, where all bands are either empty or totally occupied, the vertices of the triangles are unnecessary as long as we only need the volume integrals up to the Fermi energy. Clearly this implies a considerable saving in computer time. It is worth noting that we have encountered here one out of a class of special numerical integration formulae for polygons, in this case a formula of degree 2 for the triangle, using 3 points [21].

For $\varepsilon_{\min} < E < \varepsilon_{\max}$, where $\varepsilon_{\min}$ and $\varepsilon_{\max}$ are the minimum and the maximum values respectively of $\varepsilon(\boldsymbol{k})$ over the triangle, we write

$$J(E) = \int_{\varepsilon_{\min}}^{E} I(e)\,\mathrm{d}e \tag{A2.11}$$

and hence $J_\mu(E)$ may be approximated by a numerical integration of $I_\mu(E)$ over the interval $(\varepsilon_{\min}, E)$.

If we wish to preserve in $J(E)$ the accuracy obtained in the computation of $I(E)$ by the analytic quadratic approximation, we must be careful in the evaluation of (A2.11). The results will be rather poor if we apply some standard technique, like the repeated trapezium or Simpson rule, or Gauss–Legendre integration, without further thought. The problem is the fact that the $I_\mu(E)$ may be infinite or have an infinite and/or discontinuous derivative for some values of E. Apart from the well known van Hove singularities, singular points for a particular triangle occur at values of E where the surface $E = \varepsilon(\boldsymbol{k})$ goes through a vertex, or is tangential to a side of the triangle. A typical example

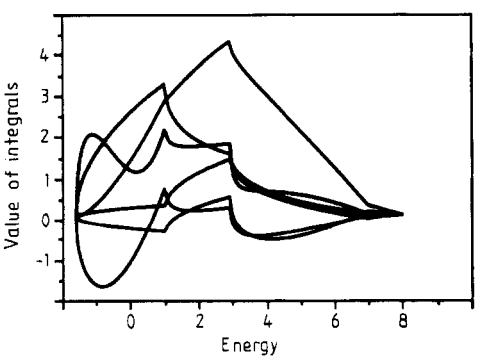

Figure A2. $I_\mu(E)$ for the six monomials μ_i. The region of integration and the dispersion relation are as mentioned in the text. Singular points occur at $E = -1.50695$, 1.109375, 3, 7 and 8.

is provided by the functions $I_\mu(E)$ depicted in figure A2; the region of integration is the triangle with vertices $(1, 2)$, $(-3, -1)$ and $(3, -2)$ and the dispersion relation is $\varepsilon(\boldsymbol{k}) = y + x^2$.

The solution to the problem is to integrate separately over the subintervals $(\varepsilon_i, \varepsilon_{i+1})$, where the ε_i are the singular points. The determination of these ε_i is a simple matter once the quadratic approximation of $\varepsilon(\boldsymbol{k})$ is known. In each of these subintervals the integrand may have an infinite derivative in the end points. To reduce the inaccuracies resulting from this aspect, a simple transformation is applied. Let the energy interval be $(0, 1)$ for the moment. Then, by the transformation

$$e = \sin^2(\pi(x + 1)/4) \tag{A2.12}$$

with

$$\mathrm{d}e = \sin(\pi(x + 1)/2)\,\mathrm{d}x \tag{A2.13}$$

this interval is mapped onto $(-1, 1)$ and the integral is rewritten as

$$\int_0^1 I(e)\,\mathrm{d}e = \int_{-1}^1 I\,[\sin^2(\pi(x + 1)/4)]\,\sin[\pi(x + 1)/2]\,\mathrm{d}x. \tag{A2.14}$$

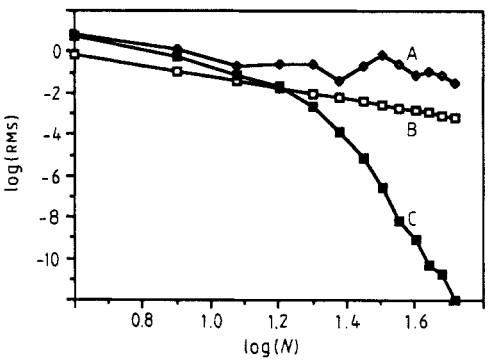

Figure A3. The root-mean-square error in $J_\mu(\varepsilon_{\max})$ resulting from numerical integration of $I_\mu(e)$ over the energy interval $(\varepsilon_{\min}, \varepsilon_{\max})$. The average is taken over the six monomials μ_i. N is the total number of integration points in the whole interval. A, Straightforward integration over the whole interval; B, division in subintervals and subsequent integration; C, application of the transformation (A2.11) for each subinterval. Gauss–Legendre integration is used for each individual integral.

Now the integrand behaves much more nicely and, for example, Gauss–Legendre integration can be applied. In figure A3 the results are shown for: A, straightforward integration over the whole energy interval; B, subdivision in subintervals and subsequent integration, and C, application of the transformation (A2.12) for each subinterval.

As we see, method B is markedly better than A, but C is superior, especially in the rate of convergence.

Appendix 3. Equivalence of formulations

In this Appendix we show the well known equivalence of expressions (3) and (2) for the surface integral $I(E)$, using the methods of this paper.

The integral

$$\int_V \int f(x,y)\delta(E-\varepsilon(x,y))\,\mathrm{d}x\,\mathrm{d}y \tag{A3.1}$$

can be evaluated by a transformation from the variables (x, y) to the variables (e, u):

$$x = g(e,u) \qquad y = h(e,u) \tag{A3.2}$$

such that

$$\varepsilon(x,y) = \varepsilon(f(e,u), g(e,u)) = \varepsilon(e,u) \equiv e. \tag{A3.3}$$

This transformation gives a parametrisation of the surface $e = \varepsilon(x, y)$ in the parameter u. The integral is in this manner transformed to the one-dimensional integral (cf (15)):

$$\int_{V_u(E)} f(E,u)\left[\frac{\partial(x,y)}{\partial(e,u)}\right]_{e=E} \mathrm{d}u. \tag{A3.4}$$

Alternatively we may consider for the same integral the form (3):

$$\int_{E=\varepsilon(x,y)} \frac{f(x,y)}{|\nabla\varepsilon(x,y)|}\,\mathrm{d}S \tag{A3.5}$$

and evaluate it by the substitution [18]

$$x = g(E,u) \qquad y = h(E,u) \tag{A3.6}$$

giving

$$\int_{V_u(E)} f(E,u)\left\{\left(\frac{\partial\varepsilon}{\partial x}\right)^2 + \left(\frac{\partial\varepsilon}{\partial y}\right)^2\right\}^{-1/2}\left\{\left(\frac{\mathrm{d}g}{\mathrm{d}u}\right)^2 + \left(\frac{\mathrm{d}h}{\mathrm{d}u}\right)^2\right\}^{1/2} \mathrm{d}u. \tag{A3.7}$$

Now, since

$$\frac{\partial\varepsilon}{\partial E} = \frac{\partial\varepsilon}{\partial x}\frac{\partial x}{\partial E} + \frac{\partial\varepsilon}{\partial y}\frac{\partial y}{\partial E} \tag{A3.8a}$$

$$\frac{\partial\varepsilon}{\partial u} = \frac{\partial\varepsilon}{\partial x}\frac{\partial x}{\partial u} + \frac{\partial\varepsilon}{\partial y}\frac{\partial y}{\partial u} \tag{A3.8b}$$

and in particular

$$\partial\varepsilon/\partial E = 1 \qquad \partial\varepsilon/\partial u = 0 \tag{A3.9a}$$

$$\partial x/\partial u = \mathrm{d}f/\mathrm{d}u \qquad \partial y/\partial u = \mathrm{d}g/\mathrm{d}u \tag{A3.9b}$$

we have

$$\left(\frac{\partial\varepsilon}{\partial x}\right)^2 + \left(\frac{\partial\varepsilon}{\partial y}\right)^2 = \left\{\left(\frac{\mathrm{d}g}{\mathrm{d}u}\right)^2 + \left(\frac{\mathrm{d}h}{\mathrm{d}u}\right)^2\right\}\left(\frac{\partial x}{\partial E}\frac{\partial y}{\partial u} - \frac{\partial x}{\partial u}\frac{\partial y}{\partial E}\right)^{-2}. \tag{A3.10}$$

Substituting (A3.10) into (A3.7) leads to (A3.4), which shows that indeed the two formulations are equivalent.

References

[1] Ashcroft N W and Mermin N D 1976 *Solid State Physics* (New York: Holt-Saunders)
[2] Gilat G and Raubenheimer L J 1966 *Phys. Rev.* **144** 390
[3] Jepsen O and Andersen O K 1971 *Solid State Commun.* **9** 1763
[4] Lehmann G and Taut M 1972 *Phys. Status Solidi* b **54** 469
[5] Rath J and Freeman A J 1975 *Phys. Rev.* B **11** 2109
[6] Kaprzyk S and Mijnarends P E 1986 *J. Phys. C: Solid State Phys.* **19** 1283
[7] Kurganskii S I, Dubrovskii O I and Domashevskaya E P 1985 *Phys. Status Solidi* b **129** 293
[8] Ashraff J A and Loly P D 1987 *J. Phys. C: Solid State Phys.* **20** 4823
[9] Mueller F M, Garland J W, Cohen M H and Benneman K H 1971 *Ann. Phys., NY* **67** 19
[10] Gilat G 1972 *J. Comput. Phys.* **10** 432
[11] Reser B I 1983 *Phys. Status Solidi* b **116** 31
[12] Cooke J F and Wood R 1972 *Phys. Rev.* B **5** 1276
[13] Chen A B 1977 *Phys. Rev.* B **16** 3291
[14] MacDonald A H, Vosko S H and Coleridge P T 1979 *J. Phys. C: Solid State Phys.* **12** 2991
[15] Methfessel M S, Boon M H and Mueller F M 1983 *J. Phys. C: Solid State Phys.* **16** L949
[16] Boon M H, Methfessel M S and Mueller F M 1986 *J. Phys. C: Solid State Phys.* **19** 5337
[17] Methfessel M S, Boon M H and Mueller F M 1987 *J. Phys. C: Solid State Phys.* **20** 1069
[18] Eisenhart L P 1947 *Introduction to Differential Geometry* (Princeton, NJ: Van Nostrand)
[19] Jansen H J F and Freeman A J 1984 *Phys. Rev.* B **30** 561
[20] Stroud A H 1971 *Approximate Calculation of Multiple Integrals* (Englewood Cliffs, NJ: Prentice-Hall)
[21] Nooyen M, te Velde G and Baerends E J *SIAM J. Numer. Anal.* submitted